Supplementary Material:

Expanded Methods:

Differential expression analysis

Differential expression was determined using the R/DESeq2 package(1) including the log2 fold change shrinkage estimation "apeglm" algorithm(2). Genes were considered differentially expressed at an adjusted p-value of < 0.05. The analysis was performed on the raw count tables (outliers already removed) with correction of covariates (age, batch, time2blood) in the model formula. Outliers were identified by sample clustering based on batch-corrected variance-stabilized expression, leading to exclusion of sample 4044 (stroke patient) small RNA sequencing experiment.

The count-change metric

The log-fold change metric is not ideally suited for assessing the potential impact of expression changes for individual miRs, because it does not reflect mean expression levels. We calculated the count-change for individual miRs and tRFs by combining base mean expression with the de-logarithmized fold-change (from DESeq2 output).

$$CC = (BM \times 2^{LFC}) - BM$$

CC: countChange, BM: baseMean, LFC: log2-fold change

Small RNA targeting predictions

Since no comprehensive tRF targeting predictions are available, we performed our own prediction based on all tRFs detected with more than 10 reads on average. We used the TargetScan 7.0(3) algorithm to determine putative miR-like binding of any 7-nucleotide substring ("seed") of any tRF to any human transcript 3'-UTR. Hits were scored according to conserved branch length (BL) and probability of conserved targeting (PCT) across all 23 available species(4) and were entered into miRNeo (seed-gene targeting and tRF-seed association).

Gene set compilation of cholinergic and associated genes

We started out with a set of 28 cholinergic genes described in(5), targets including ACYLY, CHAT, VAChT (aka SLC18A3), the 16 nicotinic and 5 muscarinic receptor subtypes, ACHE, BCHE, PRIMA1, and HACU (aka SLC5A7). In addition, we added several groups of genes known to be associated with cholinergic functioning and of interest to our aims. These comprise: genes from the neurokine and neurotrophin signaling pathways; families of genes implicated in the development and differentiation of cholinergic cell types, including lim-homeobox transcription factors, bone morphogenetic protein family genes, and genes from the JAK-STAT pathway; genes that have been associated with cholinergic function in disease, and genes implicated in splicing regulation of cholinergic transcripts.

miRs were considered Cholino-miRs if they were validated or predicted (with a score > 5/10) to target at least 5 transcripts on this list; tRFs were considered Cholino-tRFs if they contained a seed targeting evolutionarily conserved binding sites in at least 5 transcripts on this list (Supplementary Figure S2 for empirical cumulative distribution function, ECDF plot); because of diverging numbers between miRNAs and tRFs we chose to use the higher (more stringent) threshold for miRs. Transcription factors were associated with each transcript on the list in a similar manner, using the transcription factor activity derived from(6) in circulatory immune cells.

Permutation targeting analysis

Where appropriate, we determined permutation p-values via miRNeo targeting permutation. We determined a score for the test condition (e.g. by summing the individual targeting scores of all DE miRs towards cholinergic genes) and compared it to a null distribution consisting of permutated scores resulting from random substitution of test parameters (e.g. a random selection out of all genes the same size as the cholinergic test set), the p-value being the fraction of the null distribution at least as extreme as the real score.

Gene Ontology Analyses

We performed GO analyses on differentially expressed long RNA transcripts based on their differential expression p-value. GO analyses were performed using R/topGO as recommended by the authors, using the weighted method(7). Transcripts were ranked by p-value, and all DE transcripts (adjusted p-value < 0.05) with absolute log2 fold changes > 1.4 were tested against the background of the topmost

two thousand transcripts. While GO enrichment analysis can be informative, interpretation and visualization of its results is not standardized and often limited to presentation of top *X* terms by p-value. R/gsoap(8) is an analysis tool proposed to aid in interpretation of GO enrichment results via t-SNE display of similarity of terms based on the amount of shared significant genes. GO enrichment results were processed to fulfil gsoap input criteria and visualized using R/ggplot2(9).

PCR quantification of inflammatory markers after LPS stimulation

18h after LPS stimulation cells were collected in TRI-Reagent (Sigma Aldrich, St. Louis, USA) and total RNA, including small RNAs isolated using miRNeasy (Qiagen, Hilden, Germany), cDNA was synthesized from 100ng RNA using qScript™ cDNA Synthesis Kit (Quanta Biosciences, Beverly MA, USA). Expression of Cd14, Stat1, Tnf-α and Il-10 were assessed using PerfeCTa® SYBR® Green FastMix®, Low ROX™ (Quanta Biosciences, Beverly MA, USA) and normalized using Peptidylprolyl isomerase A (ppia) and 18S ribosomal RNA genes as house-keeping. Primer sequences were as follows:

Cd14: **FORWARD** AGCACACTCGCTCAACTTTTC,

REVERSE GCCCAATTCAGGATTGTCAGAC

Stat1:**F** TCACAGTGGTTCGAGCTTCAG, **R** CGAGACATCATAGGCAGCGTG

Tnf-α: **F** CCTGTAGCCCACGTCGTAG, **R** GGGAGTAGACAAGGTACAACCC

Il-10: **F** GCTCTTACTGACTGGCATGAG, **R** CGCAGCTCTAGGAGCATGTG

Ppia **F** GAGCTGTTTGCAGACAAAGTTC, **R** CCCTGGCACATGAATCCTGG

18S rRNA: **F** CTCAACACGGGAAACCTCAC, **R** CGCTCCACCAACTAAGAACG

PCR quantification of tRFs

First, we performed size selection of total RNA, to exclude molecules >25 nt in case of human samples and > 50 nt in case of cell culture experiments with RAW 264.7 cells. 1 μg was loaded into 15% TBE-Urea-Polacrylamide gel (Biorad, Hercules, USA) after mixing 1:1 with Gel Loading Buffer II (Thermo Fisher, Waltham, USA) and ran at 200V for 40-50 minutes. Gels were stained with SYBR Gold (Thermo Fisher, Waltham, USA) and visualized on UV table to cut out the desired gel piece. As size markers microRNA marker (New England Biolabs, Ipswitch, USA) and Low Range ssRNA ladder (NEB, Ipswitch, USA) were used. Afterwards, the gel fragments were incubated in 810μl 3M NaCl over-night at 4°C on

a rotation stand. Next day, the supernatant was transferred into a new Eppendorf and 1 volume of isopropranol added. After 24h at -20°C, precipitation of RNA following standard protocols was performed.

RNA concentrations were measured using Bioanalyzer (Agilent, Santa Clara, USAμ) and cDNA was prepared from 500 pg (250 pg for control samples number 16 and 18 yielding low concentrations after size selection) using qScript™ microRNA cDNA Synthesis Kit (Quanta Biosciences, Beverly MA, USA) in 20 or 40 μl, depending on the RNA concentration and diluted to 200 μl total. The levels of tRFs were determined using quantitative reverse transcription PCR (RT-qPCR) with PerfeCTa® SYBR® Green FastMix®, Low ROX™ (Quanta Biosciences, Beverly MA, USA) and normalized to hsa-miR-30d-5p, hsa-let-7d-5p, hsa-miR 106b-3p and hsa-miR 3615 (human stroke patients) or mmu-miR-30d-5p, mmu-let7d-5p for experiments with RAW 264.7 cells. Primer sequences are listed below:

hsa/mmu-miR 30d-5p: TGTAAACATCCCCGACTGGAAG

hsa/mmu-let7d-5p: AGAGGTAGTAGGTTGCATAGTT

hsa-miR-106b-3p: CCGCACTGTGGGTACTTGCTGC

hsa-miR-3615: TCTCTCGGCTCCTCGCGGCTC

tRF-22-WEKSPM852: TCGATCCCCGGCATCTCCACCA

tRF-22-WE8SPOX52 (and tRF-21-WE8SPOX5D): TCGATTCCCGGCCAATGCACC

tRF-18-8R6Q46D2: TCCCCGGCATCTCCACCA

tRF-22-8EKSP1852: TCAATCCCCGGCACCTCCACCA

tRF-18-8R6546D2: TCCCCGGCACCTCCACCA

tRF-18-HR0VX6D2: ATCCCACCGCTGCCACCA

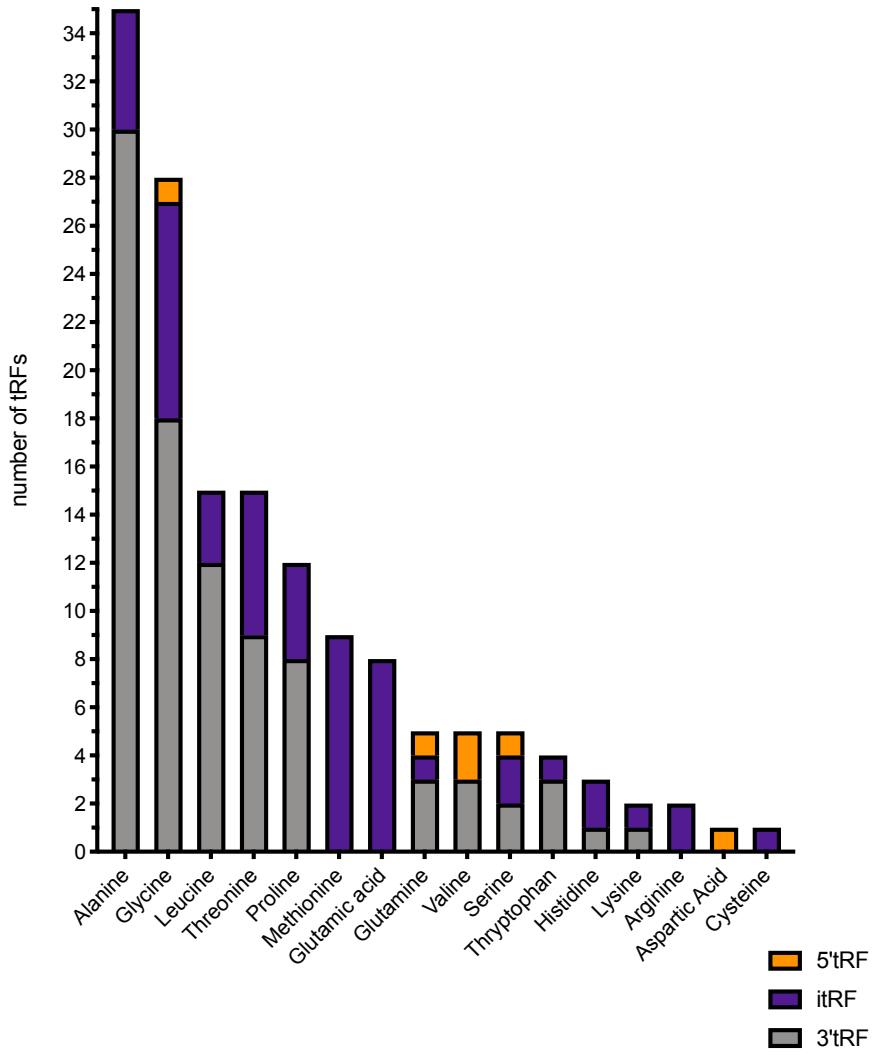

Supplementary Figure S1

Analysis of types of DE tRFs indicates non-random cleavage of tRNA molecules.

Most DE tRFs were derived from tRNAAla (35) and 3-tRFs were the most common type in the whole DE dataset.

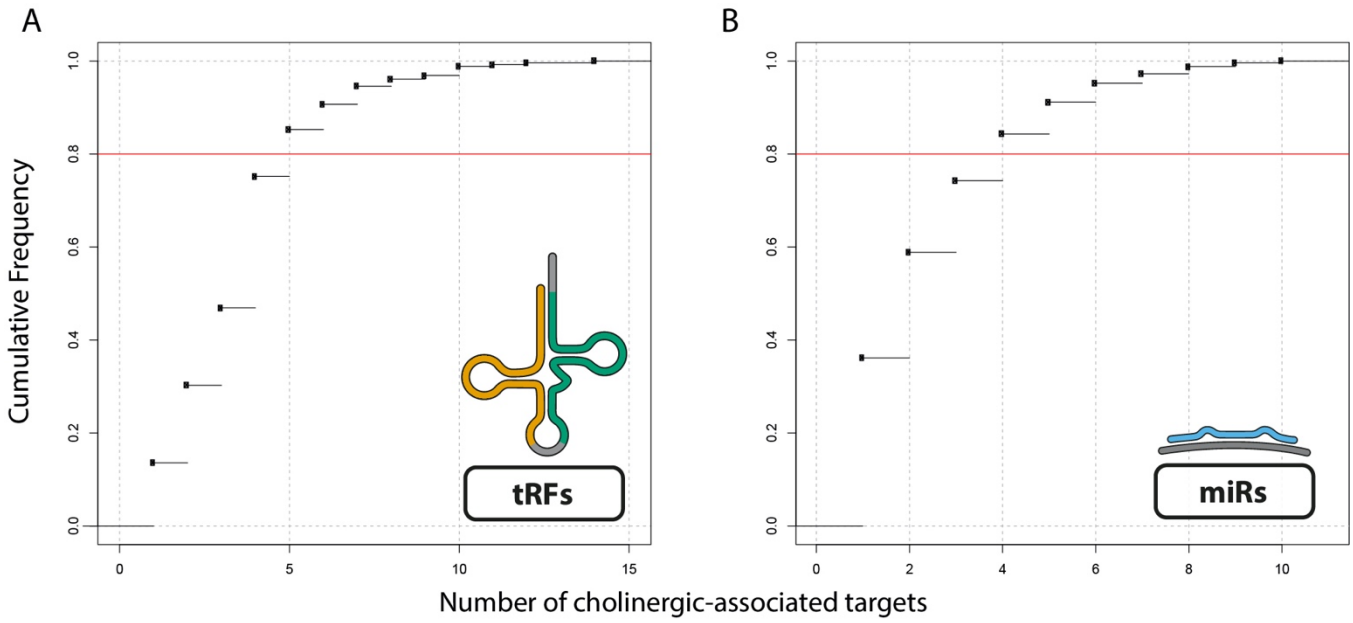

Supplementary Figure S2

Cholinergic-associated small RNA ECDF curves.

Cholinergic association was tested using miRNeo targeting data of miRs and tRFs.

To assess the best-suited threshold for defining cholinergic association, empirical cumulative density functions were calculated for the number of cholinergic-associated (CA) genes targeted by each unique small RNA. A) Cumulative frequency of number of CA genes targeted by tRFs. Threshold of 80% (red line) is passed at five CA genes targeted. B) Cumulative frequency of number of CA genes targeted by miRNAs. Threshold of 80% (red line) is passed at four CA genes targeted.

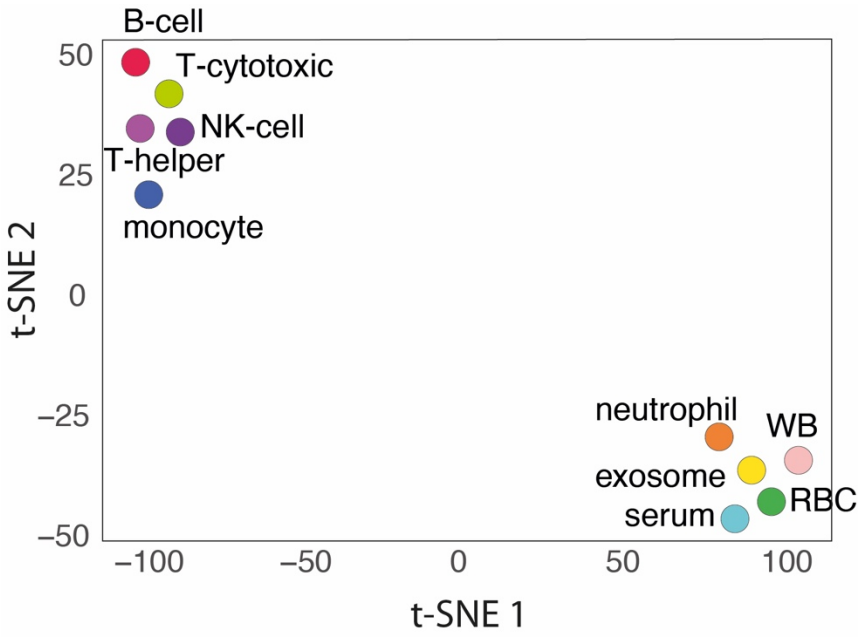

Supplementary Figure S3

tRF profiles of blood compartments distinguish leukocytes excluding neutrophils from neutrophils, erythrocytes, and non-cellular compartments. t-SNE of specific blood compartments based on tRF expression, WB – whole blood, RBC - erythrocytes

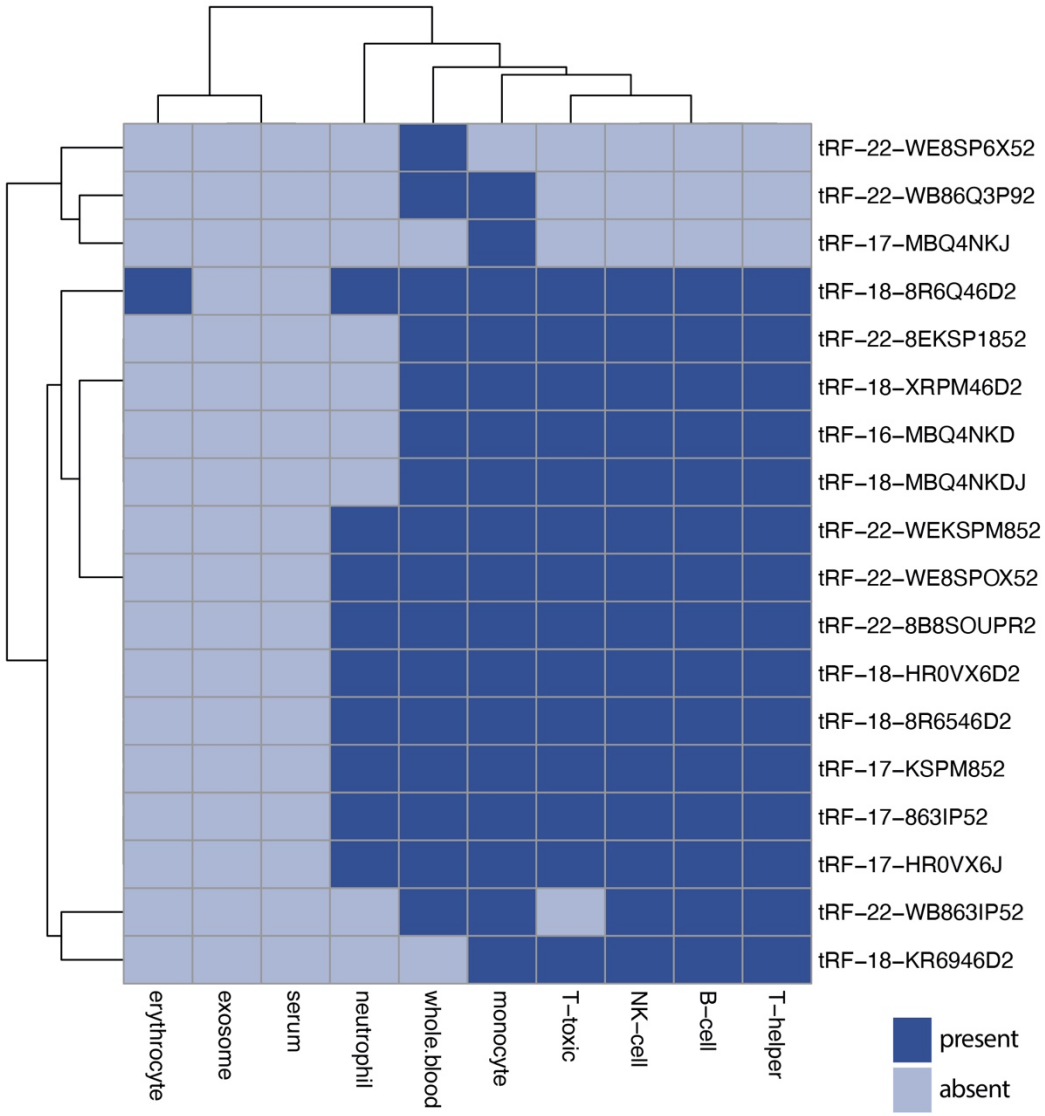

Supplementary Figure S4

Most of top 20 stroke DE tRFs are present in immune cell compartments. Heatmap showing the presence/absence of specific tRFs in defined blood compartment.

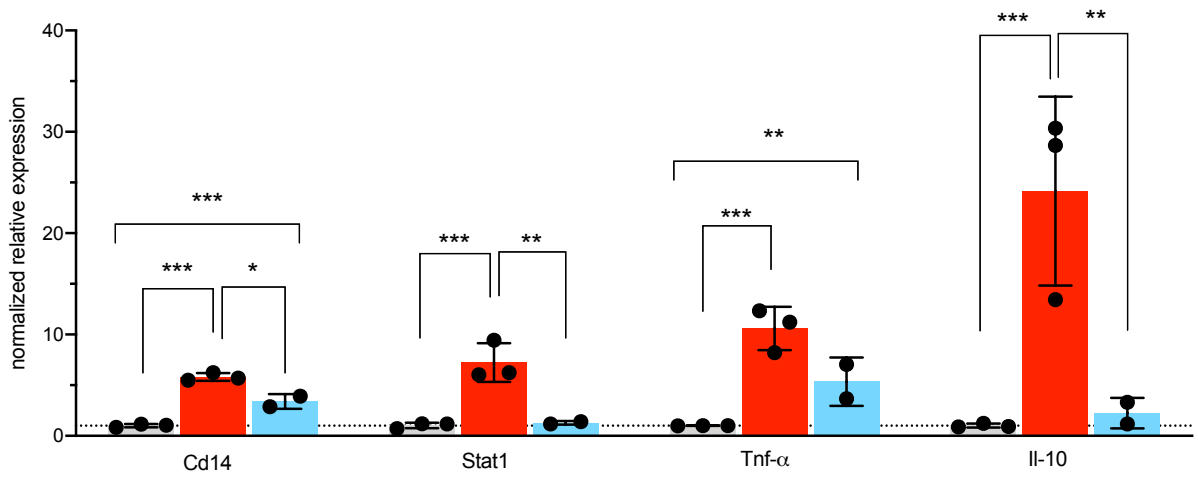

Supplementary Figure S5

Inflammatory signaling molecules and cytokines are upregulated upon 18h LPS stimulation of murine RAW 264.7 cells. Levels of Cd14, signal transducer and activator of transcription (Stat1), tumor necrosis factor alpha (Tnf-α) and interleukin 10 (Il-10) were measured with RT-qPCR using normalized expression (Ppia and 18SrRNA were used as house-keeping), relative to the unstimulated control group (line at mean normalized expression for the control group =1), Each dot represents 2-4 technical replicates, ANOVA with Tukey post-hoc, * $p < 0.05$, ** $p < 0.01$, *** $p < 0.001$, bar graphs +/- SD.

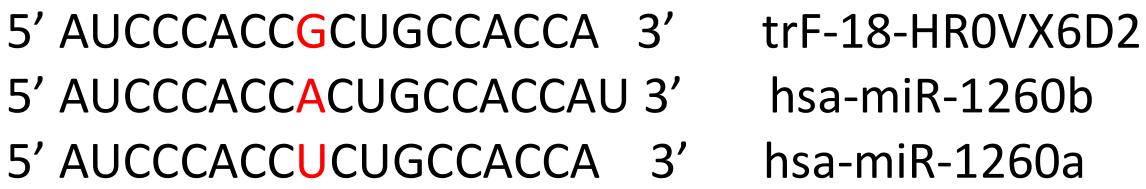

Supplementary Figure S6

Sequence of tRF-HR0VX6D2 shows high similarities to two known miRs (10)

miR-1260b differs from tRF-18-HR0VX6D2 by one nucleotide at position 9 and an additional nucleotide at the 3'-end, miR 1260a differs from tRF-18-HR0VX6D2 only at position 9.

	GO.ID	Term	Annotated	Significant	Expected	Rank in classic	classic	weight
6	GO:0001819	positive regulation of cytokine producti...	66	14	4.38	42	6.0e-05	0.00017
7	GO:0032479	regulation of type I interferon producti...	29	8	1.93	52	0.00039	0.00039
8	GO:0001818	negative regulation of cytokine producti...	51	11	3.39	51	0.00034	0.00057
9	GO:0009617	response to bacterium	95	18	6.31	35	2.5e-05	0.00059
10	GO:0045087	innate immune response	151	38	10.03	1	9.1e-15	0.00197
11	GO:0098586	cellular response to virus	15	5	1	65	0.00208	0.00208
12	GO:0046683	response to organophosphorus	22	6	1.46	68	0.00233	0.00233
13	GO:0002753	cytoplasmic pattern recognition receptor...	10	4	0.66	70	0.00284	0.00284
14	GO:0048661	positive regulation of smooth muscle cel...	16	5	1.06	72	0.00286	0.00286
15	GO:0060760	positive regulation of response to cytok...	16	5	1.06	73	0.00286	0.00286
16	GO:0014074	response to purine-containing compound	23	6	1.53	75	0.00299	0.00299
17	GO:0032649	regulation of interferon-gamma productio...	17	5	1.13	80	0.00384	0.00384
18	GO:0016525	negative regulation of angiogenesis	12	4	0.8	88	0.00603	0.00603
19	GO:0034446	substrate adhesion-dependent cell spread...	13	4	0.86	93	0.00827	0.00827
20	GO:0032496	response to lipopolysaccharide	46	8	3.06	96	0.00917	0.00917
21	GO:0009063	cellular amino acid catabolic process	14	4	0.93	100	0.01099	0.01099
22	GO:0031349	positive regulation of defense response	58	11	3.85	61	0.00109	0.01236
23	GO:0002576	platelet degranulation	22	5	1.46	102	0.01252	0.01252
24	GO:0010469	regulation of signaling receptor activit...	49	8	3.26	103	0.01340	0.01340
25	GO:0070887	cellular response to chemical stimulus	404	54	26.84	19	6.2e-09	0.01563
26	GO:0030168	platelet activation	32	6	2.13	111	0.01641	0.01641
27	GO:0034109	homotypic cell-cell adhesion	16	4	1.06	112	0.01802	0.01802
28	GO:0050731	positive regulation of peptidyl-tyrosine...	25	5	1.66	117	0.02152	0.02152
29	GO:0048469	cell maturation	17	4	1.13	118	0.02238	0.02238
30	GO:0097696	STAT cascade	17	4	1.13	119	0.02238	0.02356
31	GO:0043330	response to exogenous dsRNA	10	3	0.66	123	0.02429	0.02429
32	GO:0071695	anatomical structure maturation	18	4	1.2	127	0.02734	0.02734
33	GO:0050680	negative regulation of epithelial cell p...	19	4	1.26	139	0.03290	0.03290
34	GO:0007267	cell-cell signaling	146	11	9.7	649	0.37575	0.03503
35	GO:0001936	regulation of endothelial cell prolifera...	20	4	1.33	145	0.03907	0.03907
36	GO:0006906	vesicle fusion	20	4	1.33	146	0.03907	0.03907
37	GO:0007160	cell-matrix adhesion	20	4	1.33	147	0.03907	0.03907
38	GO:0030856	regulation of epithelial cell differenti...	12	3	0.8	151	0.04041	0.04041
39	GO:0034113	heterotypic cell-cell adhesion	12	3	0.8	152	0.04041	0.04041
40	GO:0042130	negative regulation of T cell proliferat...	12	3	0.8	153	0.04041	0.04041
41	GO:0051668	localization within membrane	12	3	0.8	154	0.04041	0.04041

Supplementary Table 1

Post-stroke DE genes are enriched in circulation- and immunity-related pathways

Full list of GO terms used for generation of tSNE in Figure 4

References:

1. M. I. Love, W. Huber, S. Anders, Moderated estimation of fold change and dispersion for RNA-seq data with DESeq2. *Genome Biol.* **15** (2014).
2. A. Zhu, J. G. Ibrahim, M. I. Love, Heavy-tailed prior distributions for sequence count data: removing the noise and preserving large differences. *Bioinformatics* **35**, 2084–2092 (2019).
3. V. Agarwal, G. W. Bell, J. W. Nam, D. P. Bartel, Predicting effective microRNA target sites in mammalian mRNAs. *Elife* **4** (2015).
4. R. C. Friedman, K. K. H. Farh, C. B. Burge, D. P. Bartel, Most mammalian mRNAs are conserved targets of microRNAs. *Genome Res.* **19**, 92–105 (2009).
5. H. Soreq, Checks and balances on cholinergic signaling in brain and body function. *Trends Neurosci* **38**, 448–458 (2015).
6. D. Marbach, *et al.*, Tissue-specific regulatory circuits reveal variable modular perturbations across complex diseases. *Nat. Methods* **13**, 366–370 (2016).
7. A. Alexa, J. Rahnenfuhrer, T. Lengauer, Improved scoring of functional groups from gene expression data by decorrelating GO graph structure. *Bioinformatics* **22**, 1600–1607 (2006).
8. T. Tokar, C. Pastrello, I. Jurisica, GSOAP: a tool for visualization of gene set over-representation analysis. *Bioinformatics* (2020) https:/doi.org/10.1093/bioinformatics/btaa001.
9. H. Wickham, *ggplot2: Elegant Graphics for Data Analysis* (Springer-Verlag, 2016).
10. N. C. T. Schopman, S. Heynen, J. Haasnoot, B. Berkhout, A miRNA-tRNA mix-up: tRNA origin of proposed miRNA. *RNA Biol.* **7**, 573–576 (2010).